APPLICATION OF THE DISCRETE ORDINATE METHOD TO BUOYANCY-INDUCED RADIATING FLUIDS IN A SQUARE ENCLOSURE WITH A MOVING WALL

Alejo Sanchez
Escuela de Ingenieria Mecanica
Universidad de Merida
Merida, Venezuela

Juan C. Morales
Dept. of Mechanical Engineering
University of Texas
Austin, Texas

Antonio Campo
College of Engineering
Idaho State University
Pocatello, Idaho

ABSTRACT

This work examines the influence of thermal radiation on the mixed convection characteristics of a fluid contained in a square cavity with a moving wall. The radiative transport equation (RTE) was integrated numerically using the discrete ordinate method. The governing conservation equations were solved numerically in the entire domain by a control-volume based finite-difference method. Detailed information about the flow, temperature and radiative fields is presented through streamlines and isotherm plots. In addition, global heat transfer rates as a function of the controlling parameters are reported. Comparisons with earlier numerical results for the mixed convection cavity excluding thermally participating radiation, are made whenever possible.

NOMENCLATURE

c_p	specific heat
g	acceleration of gravity
G	irradiation
G^*	dimensionlesss G, eq. (9)
Gr	Grashof number, eq.(9)
h	local convective coefficient
$\bar{h}$	average h
i	radiant intensity
I	dimensionless i
k	thermal conductivity
K_a	volumetric absorption coefficient
Nu	local Nusselt number
$\overline{Nu}$	average Nu, eq. (14)
N_R	radiation-conduction parameter
p	pressure
P	dimensionless p, eq.(9)
Pe	Peclet number, RePr
Pr	Prandtl number, eq.(9)
q	heat flux
Re	Reynolds number, eq.(9)
t	absolute temperature
T	dimensionless t, eq.(9)
u,v	velocities in the x- and y-directions
U,V	dimensionless u,v, eq.(9)
u_o	uniform velocity of the upper plate
x,y	coordinates
X,Y	dimensionless x,y, eq.(9)
w	side of square cavity

Subscripts

c	cold
h	hot

Superscripts

C	convective
R	radiative
T	total

Greek Letters

β	volumetric coefficient of thermal expansion
ε	emissivity
μ	dynamic viscosity
ρ	density
σ	Stefan-Boltzmann constant
τ	optical thickness, eq.(9)
θ	temperature ratio, eq.(9)

INTRODUCTION

Natural convective motion is usually induced in a stationary cavity containing a fluid even for small temperature differences. Application of a uniform velocity at the upper wall of a cavity dramatically alters the buoyant flow structure showing minicells at the corners. This mixed convection scenario represents an important type of flow occurring in various branches of engineering, geophysics and environmental sciences.

The competition between viscous and gravitational forces in mixed convection problems is quantified by the mixed convection parameter Gr/Re^2 (Gebhart et al., 1988). Correspondingly, when this ratio is greater than unity, the buoyancy forces overshadows the viscous forces and as a result, forced convection is negligible. In contrast, when this ratio is less than unity, forced convection outweighs the strength of natural convection. Logically, for moderate values of Gr/Re^2 (order of magnitude one), both convection effects coexist and compete on an equal basis.

Torrance et al. (1972) published the first numerical investigation for a mixed convection driven cavity. Their pionnering work covered a range of Grashof numbers, $-10^6 < Gr < 10^6$. The Reynolds number was fixed at Re = 100 whereas the Prandtl number, Pr = 1, typified those of gases. These authors concluded that the combined effects on the flow were quite different from the effects produced by the individual convection mechanisms. Mohamad and Viskanta (1991) reported the second numerical results for a cavity driven by combined temperature gradients and an imposed lid velocity. The cavity was filled with a liquid metal (Pr = 0.005, associated with sodium and tin). Although the Grashof number was fixed at $Gr = 10^7$, a modest range of Reynolds numbers were used for both aiding and opposing flows. Certain anomalous patterns exemplified the distinct behavior of low Prandtl number fluids. The third publication on the combined influence of Re and Gr restricted to gaseous motion inside a cavity has been authored by Ramesh and Lean (1992). In this publication, the vorticity and thermal transport equations were treated as modified Helmholtz equations and later solved via the boundary integral method.

A review of the archival literature reflects that the simultaneous effects of forced convection, natural convection and thermally participating radiation in a cavity have not been studied so far and of course are not understood. In fact, the nature of this kind of complex flow is highly nonlinear and the competing mechanisms impede the use of superposition of simple flows. From a technological perspective, buoyancy and radiatively driven flows can occur in a variety of thermal energy systems operating at either extremely high or extremely low temperatures. In these specific situations, the contribution of radiative transfer may be significant relative to natural convection. Conceptually speaking, the first mechanism is effective over "long distances" and does not require high temperature gradients within the fluid medium. On the contrary, the second mechanism is effective over "short distances" when temperature gradients exist. Consequently, these two major mechanisms may have comparable orders of magnitude in some thermal energy systems. The presence of a participating medium alters the buoyancy-driven gas flow patterns and, of course the associated temperature fields. For confined flows, the size and strength of the convective cells may be severely modified and, even destroyed. In fact, the present study is motivated by this consideration. By judicious design for a given application, the effect of a radiatively participating medium could be utilized to modify the thermal characteristics of a fluid confined to an enclosure.

In the present study, the square enclosure is filled with an absorbing, emitting and non-scattering medium which, as a first approximation, is assumed gray. Additionally, all thermophysical properties of the fluid are treated as constant, except for the buoyancy term, where the classical Boussinesq approximation has been invoked. In addition, it should be underlined that when the fluid is a radiatively participating medium, the magnitude of the optical thickness, τ, and the radiation-conduction parameter, N_R, can be envisioned as additional "radiative forces" affecting the intricate fluid motion inside the lid-driven cavity.

One of the unique features of calculating flow and heat transfer in a thermally participating gas is the choice of the radiative model. Among the approximate differential formulations that are available in the literature, the discrete ordinate method or S_N-method (Modest, 1993) has now become very popular. This preference may be attributed to a balance between its excellent accuracy and the required computational effort. In this paper, the governing conservation equations were solved with the control-volume based finite-difference formulation described by Patankar (1980). The algorithm was somewhat modified to accommodate the intrinsic features of some of the conservation equations.

This numerical study introduces for the first time a detailed local and global analysis of radiatively participating fluids confined to square cavities having a uniformly moving wall. The local analysis was done by displaying velocity, temperature and radiative fields in the computational domain. Global analysis was carried out by calculating the total, average Nusselt number of the cavity fluid flow. As a first step, this investigation focuses on a two-dimensional numerical study for mixed convection and thermal radiation.

The paper is divided into four main sections. In the first section, the physical system and the mathematical formulation is addressed. The radiative transfer equation is delineated in the second section. The third section contains a brief explanation of the computational procedure and its validation. This is followed by the last section related to the discussion of results.

DESCRIPTION OF THE PROBLEM

The physical system is illustrated in Fig. 1 and consists of a radiatively participating fluid confined to a square cavity with the upper wall moving uniformly at a velocity, u_o. The three stationary walls are maintained at uniform temperatures, T_h, whereas the moving wall is kept at a uniform temperature, T_c. The fluid is assumed as a gray medium capable of absorbing, emitting and nonscattering radiation. The flow is two-dimensional, laminar and the gravitational acceleration acts perpendicular to the moving wall. The internal surfaces of the cavity walls are gray and diffusely emitting and reflecting. The thermophysical properties of the fluid are temperature-invariant, except in the buoyancy force term where the standard Boussinesq approximation applies. Accordingly, the flow, temperature and radiative fields are described by the set of conservation equations:

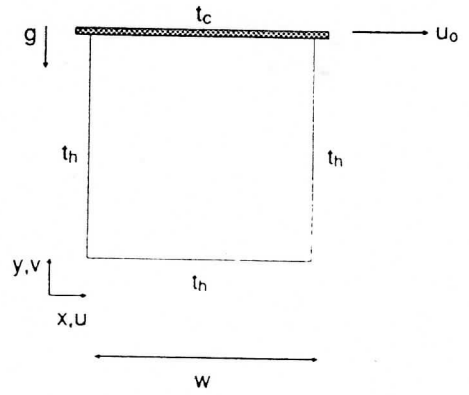

Fig. 1 Sketch of the lid-driven cavity

Mass Conservation Equation:

$$\frac{\partial(\rho u)}{\partial x} + \frac{\partial(\rho v)}{\partial y} = 0 \tag{1}$$

Momentum Conservation Equations:

x-direction:

$$\frac{\partial(\rho uu)}{\partial x} + \frac{\partial(\rho vu)}{\partial y} = -\frac{\partial p}{\partial x} + \frac{\partial}{\partial x}\left(\mu \frac{\partial u}{\partial x}\right) + \frac{\partial}{\partial y}\left(\mu \frac{\partial u}{\partial y}\right) \tag{2}$$

y-direction:

$$\frac{\partial(\rho uv)}{\partial x} + \frac{\partial(\rho vv)}{\partial y} = -\frac{\partial p}{\partial y} + \frac{\partial}{\partial x}\left(\mu \frac{\partial v}{\partial x}\right) + \frac{\partial}{\partial y}\left(\mu \frac{\partial v}{\partial y}\right) - \rho g \tag{3}$$

Energy Conservation Equation:

$$c_p\left(\frac{\partial(\rho ut)}{\partial x} + \frac{\partial(\rho vt)}{\partial y}\right) = \frac{\partial}{\partial x}\left(k \frac{\partial t}{\partial x}\right) + \frac{\partial}{\partial y}\left(k \frac{\partial t}{\partial y}\right) - div\, q^R \tag{4}$$

where the divergence of the radiative heat flux q^R is given by

$$-div\, q^R = K_a\left(G - 4\sigma t^4\right) \tag{5}$$

since

$$G = \int_{4\pi} i\, d\omega \tag{6}$$

The radiant intensity, i, appearing in eq. (6) has to be determined from the solution of the Radiative Transfer Equation (RTE) (Modest, 1993), yielding the 2-D radiative field.

THERMAL RADIATIVE MODEL

In order to carry out the computations in a convective-radiative problem, it is usually necessary to implement an unavoidable iterative approach in which the integral terms and the differential terms of the energy conservation equation, eq. (4), are solved consecutively. Naturally, the numerical solution of this intricate equation is quite involved and requires large amounts of computing time and computer storage.

Alternatively, in order to circumvent this elaborate computational procedure, one of the approximate differential methodologies, the discrete ordinate method, or S_N-method will be employed here. The discrete ordinate method solves the equation of transfer into a number of discrete angular directions spanning the total solid angle of 4π. This systematic procedure results in a set of coupled partial differential equations for the radiant intensity, i, which can be discretized using finite-volume techniques (Patankar, 1980). The associated integrals over the angular direction can conveniently be replaced by numerical quadratures. The number of discrete directions and resulting partial differential equations in the system of PDE depends on the order of the discrete-ordinate approximation, S_N. Accordingly, the S_2, S_4 and S_6 approximations correspond to 8, 24 and 48 discrete angular directions, respectively.

$$(\Omega \cdot \nabla)\, i\,(r, \Omega) = \mu_1 \frac{\partial i}{\partial x} + \mu_2 \frac{\partial i}{\partial y} = K_a\left[i\,(r, \Omega) - i_b\,(r)\right] \tag{7}$$

where μ_1 and μ_2 are the direction cosines between direction Ω and the coordinates axis.

Boundary Conditions:

The flow boundary conditions are based on the assumption that the surfaces are impermeable. Additionally, the non-slip velocity applies at the three stationary walls, and at the upper wall which moves with a uniform velocity. Therefore, the computational domain does not possess symmetry and inevitably has to coincide with the physical domain. The imposed boundary conditions are condensed in the accommpanying table

Location	u	v	t
x = 0	0	0	t_h
x = w	0	0	t_h
y = 0	0	0	t_h
y = w	u_o	0	t_c

In order to complete the set of boundary conditions, the radiant intensity, i, for each surface may be computed from the relation

$$i\,(r, \Omega) = \varepsilon\, i_b\,(r) + \frac{1-\varepsilon}{\pi} \int_{\hat{n} \cdot \Omega' < 0} |\hat{n} \cdot \Omega'|\, i\,(r, \Omega')\, d\omega \tag{8}$$

Here, the LHS is the energy leaving the surface, the first term of the RHS is the emitted energy from the surface, and the second term of the RHS is the reflected incoming energy.

BASIC EQUATIONS

The set of conservation equations has been rendered dimensionless by using the side of the cavity, w, as the scale factor for length and appropriate scale factors for the field variables: velocity, pressure, temperature and irradiation. Correspondingly, the dimensionless variables, parameters and groups are defined by

$$X = \frac{x}{w} \qquad Y = \frac{y}{w} \qquad U = \frac{u}{u_o} \qquad V = \frac{v}{u_o}$$

$$T = \frac{t - t_c}{t_h - t_c} \qquad P = \frac{p}{\rho u_o^2} \qquad G^* = \frac{G}{4\sigma t^4} \qquad I = \frac{i}{4\sigma t^4}$$

$$Pr = \frac{\mu c_p}{k} \qquad \mathrm{Re} = \frac{\rho u_o w}{\mu} \qquad Gr = \frac{\rho^2 g \beta (t_h - t_c) w^3}{\mu^2} \tag{9}$$

$$\tau = K_a w \qquad N_R = \frac{\sigma t_h^3 w}{k} \qquad \phi = \frac{t_c}{t_h}$$

Here, the scale factors that have been utilized are clearly identified.

In light of the foregoing, the system of dimensionless conservation equations becomes

Mass Conservation Equation:

$$\frac{\partial U}{\partial X} + \frac{\partial V}{\partial y} = 0 \tag{10}$$

Momentum Conservation Equations:

x-direction:

$$\frac{\partial UU}{\partial X} + \frac{\partial VU}{\partial Y} = -\frac{\partial P}{\partial X} + \frac{1}{\mathrm{Re}}\left(\frac{\partial^2 U}{\partial X^2} + \frac{\partial^2 U}{\partial Y^2}\right) \tag{11}$$

y-direction:

$$\frac{\partial UV}{\partial X} + \frac{\partial VV}{\partial Y} = -\frac{\partial P}{\partial Y} + \frac{1}{\mathrm{Re}}\left(\frac{\partial^2 V}{\partial X^2} + \frac{\partial^2 V}{\partial Y^2}\right) + \frac{Gr}{\mathrm{Re}^2} T \tag{12}$$

Energy Conservation Equation:

$$\frac{\partial UT}{\partial X} + \frac{\partial VT}{\partial Y} = \frac{1}{Pe}\left(\frac{\partial^2 T}{\partial X^2} + \frac{\partial^2 T}{\partial Y^2}\right) + \frac{4\tau_w N_R}{(1-\phi)\,Pe}\left\{G^* - [(1-\phi)T + 1]^4\right\} \tag{13}$$

TABLE 1. Sensitivity analysis of the grid for Gr = 0 using $-\psi_{max}$ as a criterion

Re	12x12	22x22	32x32	42x42	82x82
100	0.0873	0.0977	0.1000	0.102	0.103
400	0.0665	0.0850	0.0984	0.101	0.110

As may be observed in the preceding equations, the thermal buoyancy in the y-momentum equation as well as the thermal radiation in both the energy equation and the radiative transfer equation contribute to the coupling between the conserved quantities.

The set of equations, eqs. (10-13) has been solved numerically in conjunction with the system of partial differential equations generated by the various S_N approximations of the discrete ordinate method.

Ultimately, for heat transfer calculations, the total, average Nusselt number, $\overline{Nu}^T$, is conveniently defined by the additive relation

$$\overline{Nu}^T = \overline{Nu}^C + \overline{Nu}^R \tag{14}$$

where $\overline{Nu}^C$ and $\overline{Nu}^R$ identify the convective and radiative components of the Nusselt number, respectively. Each of the average Nusselt number is obtained by integrating the local values of Nu in the x- and/or the y-coordinate directions.

NUMERICAL COMPUTATION AND VALIDATION

The dimensionless conservation equations were accommodated into a general diffusion-convection type of equation and solved by the control-volume procedure (Patankar, 1980). The algorithm was somewhat modified to handle the different source terms appearing in the discretized conservation equations. In addition, the SIMPLER algorithm (Patankar, 1980) was utilized for the pressure-velocity coupling, as well as the block correction procedure of Settari and Aziz (1973) to enhance the convergence of the iterative procedure. The computer code was designed to solve a combined heat transfer problem in absorbing and emitting media with reflecting boundaries.

Relevant tests pertaining to the limiting situation of a non-radiating fluid, but for comparable conditions are indispensable. Hence, the controlling parameters of this kind of cavity problem are only three: Reynolds, Grashof and Prandtl numbers. At the beginning, uniform intervals were considered to establish grid independent results under the preponderance of forced convection (Gr = 0) for gaseous media (Pr = 0.7). Table 1 summarizes the comparison of the maximum stream function for two different Reynolds numbers, Re = 100 and 400 starting with a coarse grid of 12x12. It is important to mention that the results associated with two finer meshes of 42x42 and 82x82 were also compared and revealed minor differences (relative error = 8%) in the streamlines. Therefore, it was assumed that the 42x42 mesh was sufficiently fine and the predictions were found to be accurate, dependable and consistent. Additionally, solutions obtained for a non-radiating fluid have been compared in Table 2 against the benchmark calculations of Torrance et al. (1972) and Schreiber and Keller (1983). For practical applications, the discrepancies seem to be very

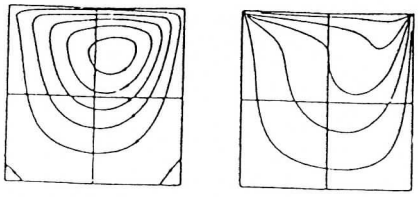

Fig. 2 Streamlines and isotherms for pure forced convection, Gr = 0

small for both Reynolds numbers tested. Therefore, the success of the code in simulating mixed convection flows of nonradiating fluids in 2-D enclosures has been demonstrated.

Structures of the flow and thermal fields for a non-radiating gas (Pr = 0.7) wherein Re = 100 and Gr = 0 are included in Fig. 2 primarily for comparison purposes. This particular case exemplifies a single primary eddy at the center of the cavity and small secondary eddies at the corners. Temperature fields exhibit a minute stratification where all isothermal lines are clustered in the 1/3 upper portion of the cavity. Actually, this format correlates closely with the corresponding flow and temperature patterns computed by Torrance et al. (1972).

Direction is turned now to the radiative model. Several runs were made for critical cases associated with participating radiation. A comparison of the results for both temperature and intensity using S_4 and S_6 approximations do not manifest significant changes as it is expected for an absorbing-emitting medium. In view of this, it was decided to utilize the S_4 approximations throughtout the calculations.

Numerical values of the local Nusselt numbers are calculated after convergence for the velocity, temperature and radiative fields is attained. The overall energy balance, written in terms of the integrated heat transfer rate through each wall, must be equal. Agreements to less than 1% of the total, average Nusselt number $\overline{Nu}^T$ were found for all cases ensuring the accuracy of the numerical computations.

PRESENTATION AND DISCUSSION OF RESULTS

When the medium is a radiatively participating fluid, in addition to the customary descriptive parameters: the Reynolds number, Re, the Grashof number, Gr, and the Prandlt number, Pr; the radiative parameters the optical thickness, τ, the radiation-conduction parameter, N_R, and the temperature ratio, θ, play a decisive role. Understandably, the excessive number of parameters prevented us from presentating a full-blown parametric study of the problem. Therefore, with this rectriction in mind, representative numerical results will be reported for situations connected to a single intermediate value of θ, $\theta = 0.5$. Nevertheless, additional results for other values of θ that deviate from 0.5 have been generated as well, but are not presented in order to save space.

The cavity was assumed as one with perfectly black surfaces. Calculations were performed for a primary case: Reynolds number of 100 and a Prandtl number of 0.7. Since the wall temperature ratio was kept constant, the Grashof number received positive values: $Gr = 10^4$, 10^5 and 10^6, such that the mixed convection parameter Gr/Re^2 ranged

TABLE 2. Comparison of the values of $-\psi_{max}$ for Gr = 0

Re	Present Work	Torrance et al. (1972)	Schreiber and Keller (1983)
100	0.103	0.101	0.103
400	0.110	——-	0.113

TABLE 3. Variation of the convective Nusselt number for Re = 100

$\overline{Nu}^C$	Gr
8.2595	10^3
8.4233	10^4
7.9499	2×10^4
7.7143	4×10^4
7.6987	5×10^4
7.7471	6×10^4
7.8955	7×10^4
8.2652	10^5
15.4240	10^6

from 1, 10 and 100. Thus, three different orders of magnitude for Gr/Re^2 will be examined. As already mentioned, when the fluid is not transparent, the magnitude of the optical thickness τ and the companion radiation-conduction parameter N_R can be envisioned as additional "radiative forces" affecting markedly the fluid motion. The numerical values of the radiative parameters τ and N_R have been chosen as 0.1, 1 and 10.

Influence of Natural Convection

For a transparent fluid, ($\tau = 0$), the influence of buoyancy on forced convection was studied. Computed flow and temperature fields for Grashof numbers ranging from 10^4 to 10^6 are presented in Figures 3-5. Natural convection may either aid or oppose to the main flow generated by the lid motion. At the left wall, warm buoyant fluid creates a thin boundary layer which tends to accelerated the flow near the wall (aiding) and The opposite effect is present at the right wall, where warm fluid tends to go against of the main stream (opposing). Hence, the boundary layer at the right wall separates, creating a multicellular flow. Consequently, the main flow velocity decrease.

Results for $Gr = 10^4$ shows that the buoyant flow is dominated by the force convective flow and it is confined to a small secondary flow at the right bottom corner. The isotherm plot indicates that the flow is partially stratified at the bottom of the enclosure. As the strength of buoyancy increases, $Gr = 10^5$, the bottom cell starts growing and tends to confine the driven flow to a small region just below the moving lid. Hence, the fluid motion in the driven cell is slower than the case for $Gr = 10^4$. For $Gr = 10^6$, the flow is totally dominated by the buoyancy forces and the driven flow is confined to a very thin region of high shear stress just below the lid. The presence of two

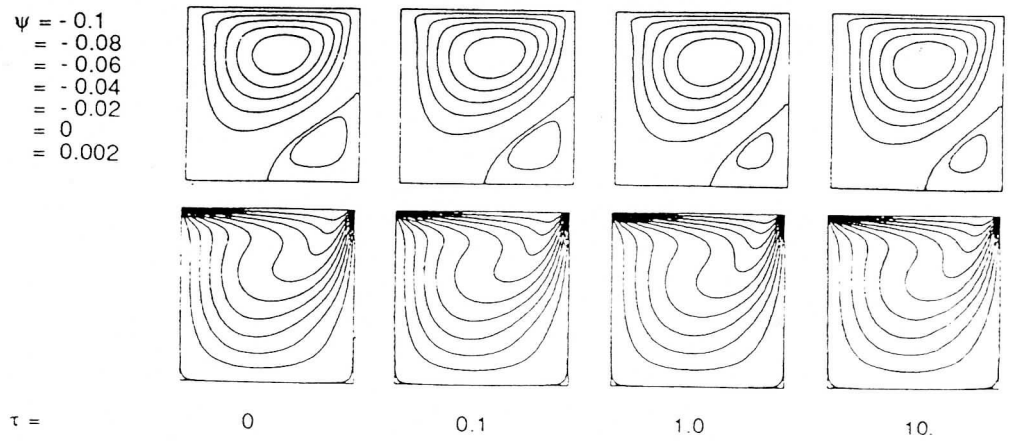

Fig 3. Streamlines and isotherms for $Gr = 10^4$ and $N_R = 1$ ($\Delta t = 0.1$)

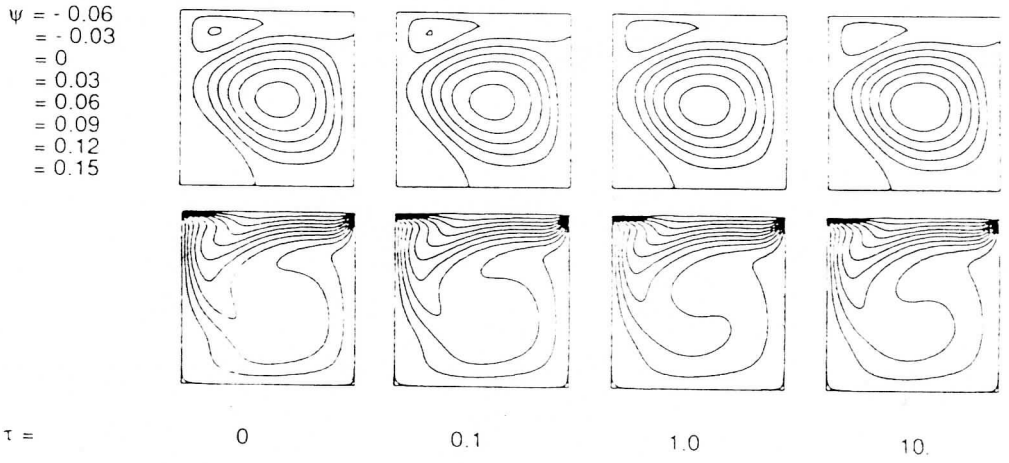

Fig 4. Streamlines and isotherms for $Gr = 10^5$ and $N_R = 1$ ($\Delta t = 0.1$)

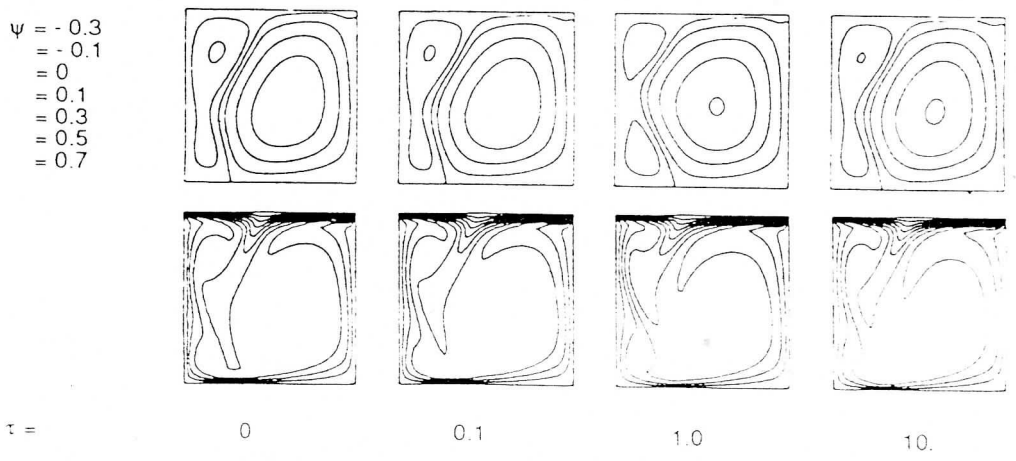

Fig 5. Streamlines and isotherms for $Gr = 10^6$ and $N_R = 1$ ($\Delta t = 0.1$)

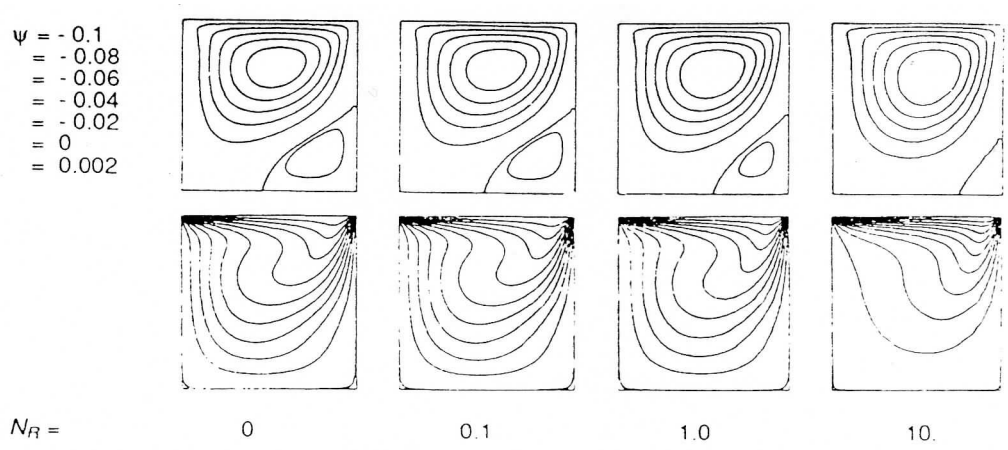

Fig 6. Streamlines and isotherms for Gr = 10^4 and τ = 1 (Δt = 0.1)

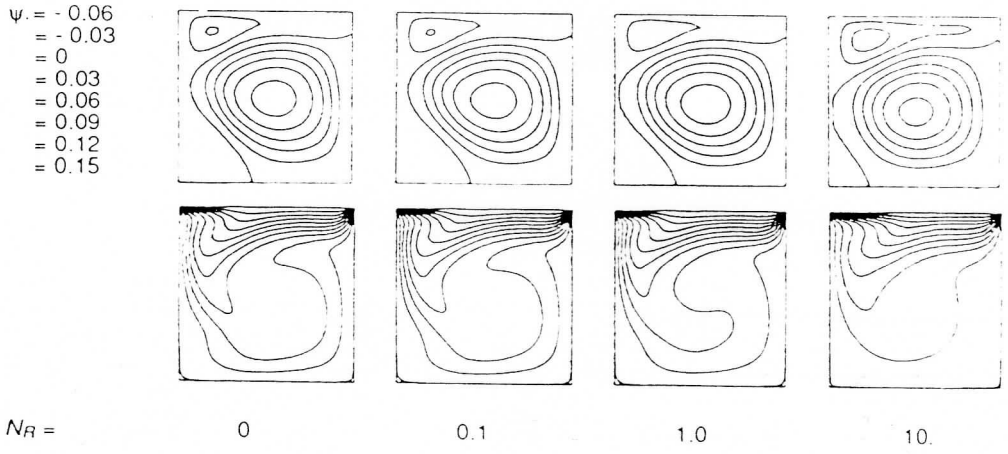

Fig 7. Streamlines and isotherms for Gr = 10^5 and τ = 1 (Δt = 0.1)

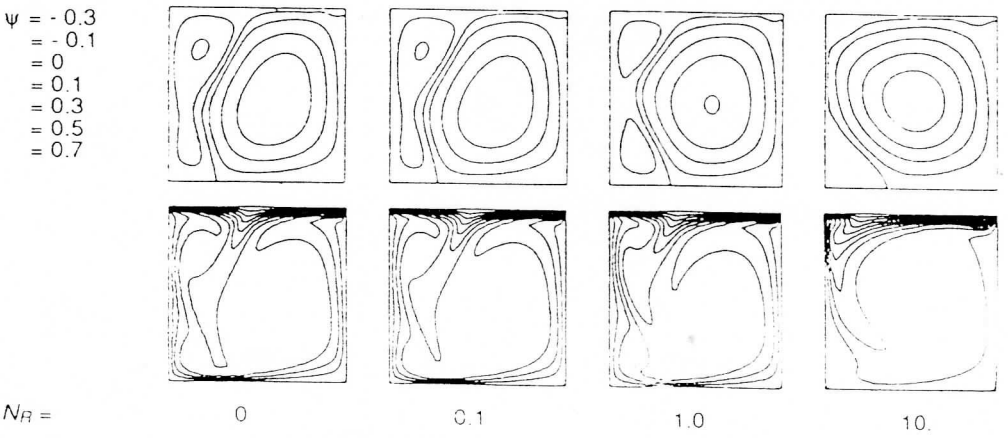

Fig 8. Streamlines and isotherms for Gr = 10^6 and τ = 1 (Δt = 0.1)

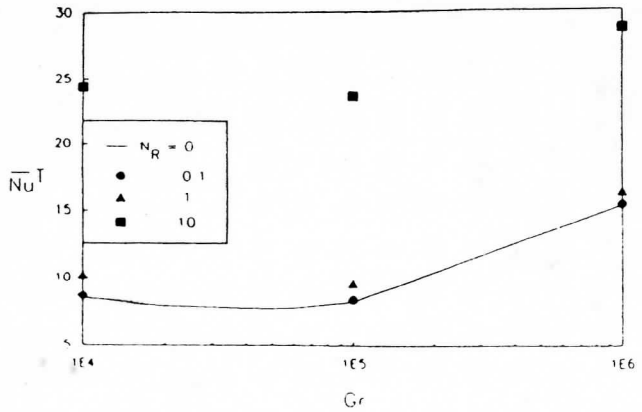

Fig. 9 Variation of the total, average Nusselt number for $\tau = 1$

contrarotating cells is similar to the case of a stationary lid and pure natural convection.

The behavior of the average Nusselt number is explained in Table 3. It may be seen that Nu shows a prevalent monotonic increasing behavior, with the exception of the region between $Gr = 10^4$ and 10^5 where a minimum value is noticeable. This is, of course, the result of the confrontation between the two competing forces as revealed in the movement of the cells.

Influence of Thermal Radiation

Computed results for the influence of thermal radiation on mixed convection are presented in Figs. 3-8. The influence of the optical thickness was studied for a constant value of the radiation-conduction parameter ($N_R = 1$) in Fig. 3-5. For $Gr = 10^4$, there is not noticeable changes on the streamlines and isotherms. In contrast, for higher Grashof numbers, $Gr = 10^4$, the flow within the right cell tends to accelerate as the optical thickness increases. However, the left cell decelerates until it reaches a minimum around $\tau = 1$ and starts accelerating for higher values of the optical thickness. As a consequence, the total heat transfer decreases as the medium starts to participate radiatively.

On the other hand, the effect of the radiation-conduction parameter is strongly marked even for low Grashof number. Results for $\tau = 1$ and values of N_R ranging from 0 to 10 are presented in graphical form, Fig. 6-8. At $Gr = 10^4$, the flow is not affected for low values of the radiation-conduction parameter, but for N_R greater than 1 the shapes of the isotherms are drastically changed, being pushed up againts the cold moving wall. Similar patterns are observed at higher Grashof numbers. Moreover, at higher Grashof numbers, the size of the right cell tends to increase as N_R increases.

Fig. 9 displays results for $\overline{Nu}^T$ versus the Grashof number maintaining $\tau = 1$. From $Gr = 10^4$ to 10^6 the impact of N_R is practically negligible, except for $N_R = 10$. The same trend persists for $Gr = 10^6$ but with more vigor.

CONCLUDING REMARKS

An in-depth numerical study was made of natural convection of radiating fluids confined to a square cavity with a moving wall. Two-dimensional simulations are employed to illustrate the fluid flow, thermal and radiative phenomena occurring in the present system. Upon adoption of the S_4 approximation of the discrete ordinate method, it was found that the flow in the majority of the cases, was characterized by multiple cells for combinations of the controlling parameters. Overall, the present results conclusively demonstrate that the presence of thermal radiation affects mixed convection processes especially for low Reynolds number flows. Under these circumstances, forced convection is weak.

Although the agreement between measured and predicted temperatures for nonradiating fluids is generally good, the results suggest that accurate numerical techniques such as the powerful S_N-method are acceptable to fully understand the complex behavior of mixed convection accounting for radiating gases in the present configuration. Finally, additional experiments should be performed covering larger ranges of Reynolds and Grashof numbers for vigorous radiating liquids. Unquestionably, this data will provide unparallel information to validate radiative models along with high-accurate computer codes.

REFERENCES

Gebhart, B., Jaluria, Y., Mahajan, R.L. and Sammakia, B., 1988, *Buoyancy-Induced Flows Transport*, Hemisphere, *New York, NY*.

Modest, M.F., 1993, *Radiative Heat Transfer*, McGraw-Hill, New York, NY.

Mohamad, A.A. and Viskanta, R., 1991, Transient Low Prandtl Number Fluid Convection in a Lid-Driven Cavity, *Numerical Heat Transfer*, Part A, Vol. 19, pp. 187-205.

Patankar, S.V., 1980, *Numerical Heat Transfer and Fluid Flow*, McGraw-Hill, New York, NY.

Ramesh, P.S. and Lean, M.H., 1992, A Boundary Integral Formulation for Natural Convection Flows, *Communications in Applied Numerical Methods*, Vol. 8, pp. 407-415.

Schreiber, R. and Keller, H.B., 1983, Driven Cavity Flows by Efficient Numerical Techniques, *Journal of Computational Physics, Vol. 49, pp. 310-333*.

Settari, A. and Aziz, K., 1973, A Generalization of the Additive Correction Methods for the Iterative Solution of Matrix Equations, *SIAM Journal of Numerical Analysis*, Vol. 10, pp. 506-521.

Torrance, K., Davis,R., Eike, K., Gill, P., Gutman, D., Hsui, A., Lyons, S. and Zien, H., 1972, Cavity Flows Driven by Buoyancy and Shear, *Journal of Fluid Mechanics, Vol. 51, pp. 221-231*